Diesel Particulate Matter and NO_x Removals Using a Pulsed Corona Surface Discharge

S. Yao, M. Okumoto, and T. Yashima
Chemical Research Group, Research Institute of Innovative Technology for the Earth, Kyoto 619-0292, Japan

J. Shimogami and K. Madokoro
Dept. of Physics, Kyoto Sanyo University, Kyoto 603-8555, Japan

E. Suzuki
Dept. of Fine Material Engineering, Shinshu University, Ueda 386-8567, Japan

A pulsed corona surface discharge (PCSD) system was established for particulate matter (PM) and NO_x removals from a diesel engine. The PCSD was carried out with a dielectric barrier discharge (DBD) reactor and a pulse power supply at atmospheric pressure and room temperature. The DBD reactor consisted mainly of an alumina (Al_2O_3) tube and a stainless steel rod (cathode) inserted in the alumina tube, and an aluminum coil (anode) wound on the outside surface of the Al_2O_3 tube. Pulse voltage was applied to the outside Al coil and stainless steel rod. PM was removed at a rate of 89% at maximum with 40% NO_x removal. Relations of pulse voltage and frequency to PM and NO_x removals were investigated. PM was oxidized by NO_2 and other kinds of active oxygen species, such as O and O_3 from plasma discharges. A surface adsorption/desorption and PM oxidation model of PM removal was established. The kinetic equations and their constants were given. © 2004 American Institute of Chemical Engineers *AIChE J,* 50: 715–721, 2004

Keywords: PM removal, NOx removal, pulsed plasma, corona surface discharge, DBD reactor, kinetic model

Introduction

Diesel engines emit particulates and nitrogen oxides (NO_x, $x = 1$ or 2) and hydrocarbons (HCs), which have been identified as toxic substances and contribute to the development of cancer; cardiovascular and respiratory health effects; pollution of air, water, and soil; reductions in visibility; and global climate change (Lloyd and Cackette, 2001). Technologies such as engine modification using exhaust-gas recirculation (EGR) and aftertreatment systems result in significant emission reductions of particulate matter (PM) and NO_x (Zelenka et al., 1996; Neeft et al., 1996; Koltsakis et al., 1997). The aftertreatment systems include mainly diesel particulate filters (DPF) for PM removal and catalysts for CO, HCs, and NO_x reductions. These aftertreatment systems can effectively reduce emissions, but need fuels with sulfur content < 15 ppmw (Inomato, 2001) and additional energy (such as fuel or electricity) (Aoyagi, 2001). DPF as well as catalyst-based DPF systems have been widely studied for PM removal with its unsolved problems such as the cost of using the DPF made from SiC (Matsuura, 2000). The aftertreatment system for NO_x removal includes the lean NO_x catalyst and selective catalytic reduction (SCR) that use a reactant such as diesel fuel, ammonia, or urea to reduce NO_x (DECSE Program Phase I Report No. 1, 1999; Phase II Summary Report, 2000; Final Report, 2001).

Nonthermal plasmas (NTP) also have been developed for gas cleanings of acid and greenhouse gases in combustion flue gases, such as NO_x, SO_x, VOC, and PM removals, and for other applications, such as methane conversion (Chang et al., 1991; Eliasson, 1991; Chang, 1993; Penetrante, 1993; Tamon

---

Correspondence concerning this article should be addressed to S. Yao at yao@rite.or.jp.

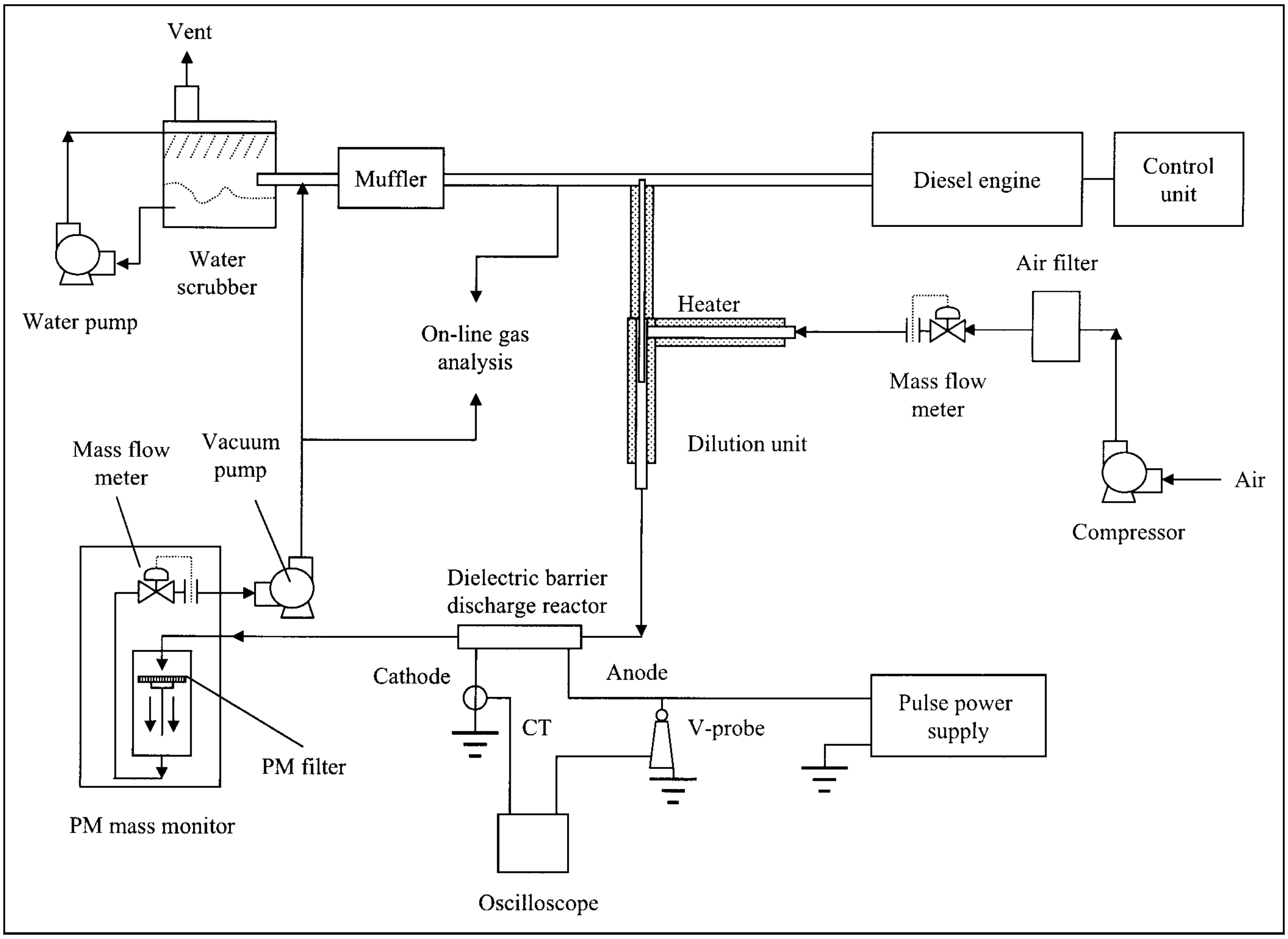

Figure 1. The diesel engine and its dynamic, pulse power supply; dielectric barrier discharge reactor, and their voltage and current measuring system; NO/NO_2 and gas composition analysis system.

et al., 1995, 1996, 1998; Liu et al., 1996; Larkin et al., 1998; Penetrante et al., 1998; Sano et al., 1998; Thanyachotpaiboon et al., 1998; Balmer et al., 1999; Doria and Kushner, 1999; Hemmingway et al., 1999; Lepperhoff et al., 1999; Thomas et al., 2000; Matsui et al., 2001). Those approaches have proposed that such nonthermal plasmas have potential for the treatment of both NO_x and PM.

In 2000, Thomas et al. used a NTP reactor in which ceramic balls are packed between two electrodes to treat PM and NO_x in exhaust gases from a Nissan 2.71 IDI diesel engine. They found that the NTP reactor has an effect on the oxidation of PM in diesel exhausts at a low temperature. However, most of the NO is converted to NO_2. This finding suggested that further treatment to convert NO_2 to NO is required, as NO_2 is more toxic than NO.

The authors recently developed a high-frequency pulsed plasma for activated carbon oxidation (Yao et al., 2001). The experimental results showed that carbon could be oxidized to CO and CO_2 at a rate of 1.1–11 μg/J-electricity, indicating that the pulsed plasma has potential for PM oxidation. In this article, a pulsed corona surface discharge (PCSD) process using a dielectric barrier discharge (DBD) reactor and a pulse power supply was developed for the removal of PM and NO_x from a diesel engine. The mechanisms of PM oxidation and NO_x reduction were proposed. A kinetic model of PM removal was established.

Experimental Setup

A 2-L (4-cylinder, 54-kW maximum output at 4700 rpm) diesel engine was installed in a hydrodynamometer test cell

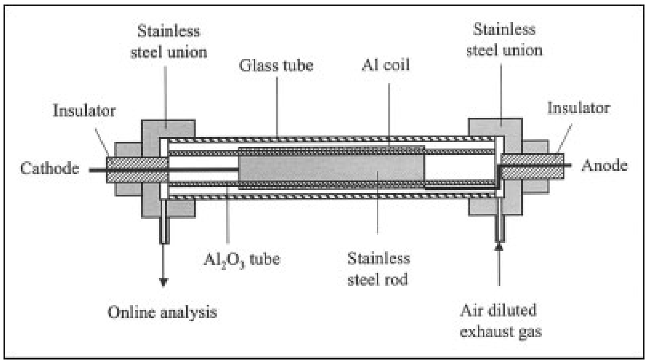

Figure 2. Structure of the dielectric barrier discharge reactor.

equipped with a performance-measurement system and a gas-analysis system (Figure 1). The main property of the diesel fuel (Japan Energy, Tokyo) was specific gravity at 15°C: 0.8357 g/cm^3; cetane number: 59.6; flash point: 94.5°C; and sulfur: 0.031 wt %. A part of the exhaust gas was diluted with air at 150°C using a dilution unit. The air-diluted exhaust gas was then cooled to room temperature and sent to the DBD reactor (Figure 2) at atmospheric pressure and without external heating except plasma heating. The outlet gas from the DBD reactor was measured on-line using a GC-103 gas chromatograph (Ohkura, FID, column: ID $\Phi 3 \times 10^{-3} \times 2$ m^2 Porapak N, a methanizer converting CO and CO_2 to CH_4 was added prior to FID) for CO and CO_2 analyses, an AGC-280 gas chromatograph (Ohkura, TCD, column: ID $\Phi 3 \times 10^{-3} \times 2$ m^2 molecular sieve 5A) for O_2 and N_2 analyses, and a NO/NO_2/NO_x analyzer (ECL-88US, Yanaco) for NO and NO_2 analyses. The PM emission rate in g/s was measured using a PM mass monitor (TEOM 1105, Rupperecht & Patashnick).

PM and NO_x removal was calculated using Eqs. 1 and 2, respectively. CO concentration increase was defined as the percentage of CO increased due to the plasma discharges, as shown in Eq. 3

$$\text{PM removal } X = \frac{\text{PM emission rate without plasmas} - \text{PM emission rate with plasmas}}{\text{PM emission rate without plasmas}} \times 100\% \quad (1)$$

$$NO_x \text{ removal} = \frac{NO_x \text{ concentration without plasmas} - NO_x \text{ concentration with plasmas}}{NO_x \text{ concentration without plasmas}} \times 100\% \quad (2)$$

$$\text{CO increase} = \frac{\text{CO concentration with plasmas} - \text{CO concentration without plasmas}}{\text{CO concentration without plasmas}} \times 100\%. \quad (3)$$

The DBD reactor (Figure 2) consisted mainly of a glass tube (1.3×10^{-2} ID $\times$ 1.5×10^{-2} OD $\times$ 0.2 m^3), an alumina (Al_2O_3) tube (6×10^{-3} ID $\times$ 1.0×10^{-2} OD $\times$ 0.2 m^3), an aluminum (Al) coil ($\Phi 5 \times 10^{-4}$ m, 68 rolls, 2.3 m length) wound spirally on the central outside surface of the Al_2O_3 tube, and a stainless steel rod (6×10^{-3} OD $\times$ 0.085 length m^2) inserted into the Al_2O_3 tube and set in the central position of the Al_2O_3 tube. The outside Al coil was used as an anode and the inside stainless steel rod as a cathode. Pulse voltage was applied between the anode and cathode using a pulse power supply (DP-10K10, Peec). The pulse power supply could generate a pulse peak voltage (V_p) of 10 kV of a rise time level of 10^{-8} s and a pulse repetition of 10 kHz at maximum. The discharge voltage and cathode current were measured with a voltage probe (EP-50K, Peec) and a current transformer (Model 2-1.0, Strangenes), respectively. The analog signals from the voltage probe and current transformer were recorded with a digital phosphor oscilloscope (TDS 7104, Tektronics). The energy injection, P, in J/pulse from the pulse power supply to the DBD reactor was calculated from the waveforms of voltage and cathode current using Eq. 4. The energy injection rate in watts was defined as the product of P and pulse frequency, F, in hertz

$$P = \sum_i (V_i I_{c_i}(t_{i+1} - t_i)). \quad (4)$$

Here, V_i and Ic_i are voltage in volts and cathode current in amperes, respectively, at discharge time, t_i, in seconds.

Energy efficiency of PM removal due to the PCSD in g/J is defined as Eq. 5:

$$\text{Energy efficiency} = \frac{\text{PM emission rate} \times \text{PM removal}}{PF} \quad (5)$$

Results and Discussion

Typical waveforms of discharge voltage and current

The typical waveforms of discharge voltage and cathode current are shown in Figure 3 at a fixed pulse frequency of 1 kHz. The pulse voltage increased to a peak voltage of 7.3 kV (V_p) within about 3.5×10^{-8} s. The cathode current increased to a peak value of 22 A simultaneously, while the voltage increased and dropped to zero within a time frame of 5×10^{-7} s, whereas the rest time was about 1×10^{-3} s over a pulse discharge duration without any discharge. This discharge cur-

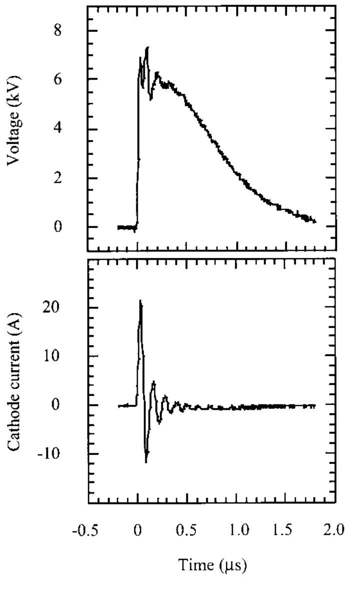

Figure 3. Typical waveforms of discharge voltage and cathode current at 1 kHz.

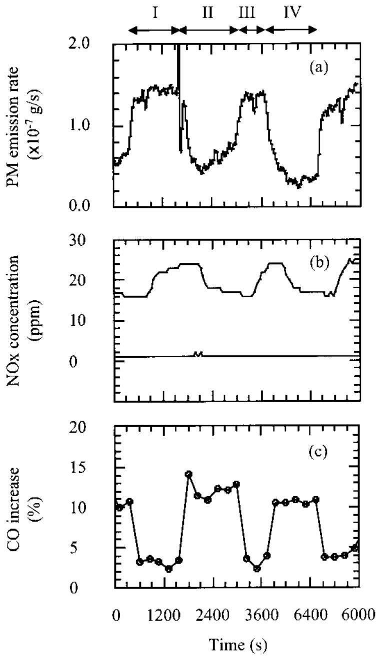

Figure 4. Typical results of PM and NO_x removals and CO concentration increase.

Zones I and III: without PCSD; Zone II, 4.4 kV (Vp) and 6 kHz; Zone IV: 5.2 kV (Vp) and 1 kHz.

rent involved the current for plasma PCSD and the current for charging stray capacitors on the DBD reactor side.

PM and NO_x removals

Exhaust gases of 6.07×10^{-6} m^3/s from the diesel engine operating at 1 krpm and 4 kW was diluted 2.9 times with filtered air at 150°C, cooled to room temperature, and introduced into the DBD reactor. The typical PM emission rate and NO, NO_2, CO, CO_2 concentrations in the gases from the DBD reactor were analyzed with or without plasma discharges (Figure 4). The PM emission rate (based on 6.07×10^{-6} m^3/s exhaust gas) was 1.44×10^{-7} g/s without plasma discharges, and decreased to a level of 4×10^{-8} g/s at 6 kHz and a peak voltage of 4.4 kV (V_p), and 3×10^{-8} g/s at 1 kHz and 5.2 kV (V_p) (Figure 4a). NO and NO_2 concentrations decreased while plasma discharges were carried out with about a 90-s delay due to long sampling tube and the small amount of sampling gases (Figure 4b).

PM is mainly composition of hydrocarbons. In order to find the products of PM under plasma discharges, an experiment was performed using a reactor similar to the DBD reactor shown in Figure 2, only an Ag coil and oxygen (10%) and nitrogen (90%) were used instead of an Al coil and air-diluted exhaust. More than 60% of PM was converted to CO_2 and less than 40% to CO. When the air-diluted exhaust gas was used, CO increased by about 10% with plasma discharges due to incomplete PM oxidation (Figure 4c). The maximum PM removal rate was 89% at a peak voltage of 6.2 kV and a pulse frequency of 1 kHz with a NO_x removal of 40% and a CO increase of about 20%.

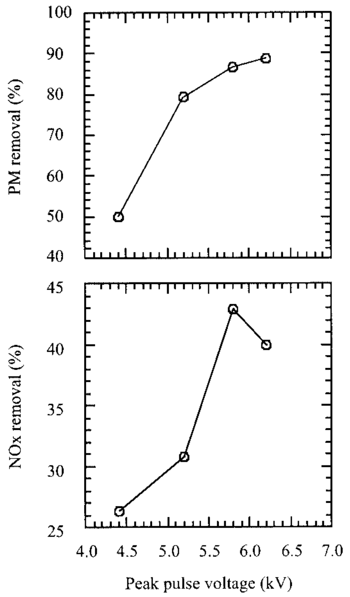

Figure 5. PM and NO_x removals as a function of peak pulse voltage at 1 kHz.

The influence of energy injection and frequency was then illustrated in Figures 5 and 6. PM removal increased by increasing the pulse's peak voltage from 50% at 4.4 kV (V_p) to 89% at 6.2 kV (V_p), indicating that the peak voltage is an important factor that contributes to PM removal. NO_x removal peaked at a peak voltage of 5.8 kV (V_p).

The pulse frequency is also an important factor affecting PM and NO_x removals. PM removal increased linearly with increasing pulse frequency up to 2 kHz and peaked at 2 kHz. NO_x removal increased with increasing pulse frequency and attained to a certain level of 36%.

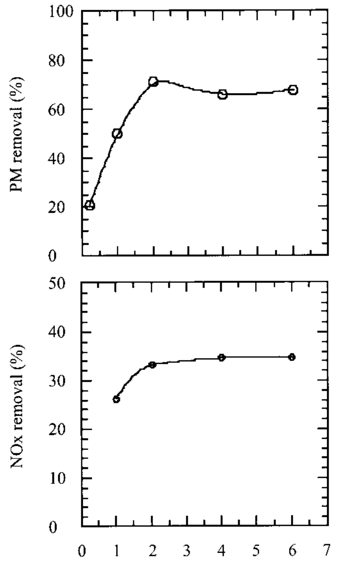

Figure 6. PM and NO_x removals as a function of pulse frequency at energy injection of 6.6×10^{-4} to 8.1×10^{-4} J/pulse.

Mechanism of PM and NO_x removal

Plasmas have been used to convert NO to NO_2 and then to N_2 over catalysts (Rappé et al., 2001) or to HNO_3 after reactions of NO_2 with such as H_2O or OH, or directly reduce NO to N_2 by N (Dorai and Kushner, 2000). Dorai et al. (2000) have studied in detail the interaction between soot particles and NO_x during DBD plasma remediation of simulated diesel exhaust. They built a surface-reaction mechanism for the removal of soot particles (denoted by C_xH_y) and NO_x; the main reactions, which are also important for this study, are listed in Eqs. 6 to 11. The removal of NO_x from the exhaust is mainly due to the oxidation of NO to NO_2 and later to HNO_3 and/or to HNO_2 after reactions such as with OH (Eqs. 6 and 7). The fraction of NO_x removal that is actually converted to HNO_2 and HNO_3 ranges between 10 and 20%, indicating that NO acts as a catalyst that accelerates PM oxidation

$$NO_2 + OH + M \rightarrow HNO_3 + M \tag{6}$$

$$NO + OH + M \rightarrow HNO_2 + M \tag{7}$$

$$C_xH_y + NO_2 \rightarrow (C_{x-1}H_y) - C - NO_2 \tag{8}$$

$$C_xH_y + NO_2 \rightarrow (C_{x-1}H_y) - C - ONO \tag{9}$$

$$C_{x-1}H_y - C - NO_2 \rightarrow C_{x-1}H_y + NO + CO \tag{10}$$

$$(C_{x-1}H_y) - C - ONO \rightarrow C_{x-1}H_y + NO + CO \tag{11}$$

A recent article by Dorai and Kushner (2002) showed that when using multiple pulses and the DBD reactor, NO_x removal was 35% at an energy deposition of 30 J/L in the absence of soot and 37% with soot. NO_x removal can be improved by the increased production of HNO_2, HNO_3, organic nitrates, and nitrites.

In this study, we have found that PM could be oxidized to CO and CO_2 in the presence of O_2, but in the absence of NO_2. This implied that other kinds of active oxygen spices except NO_2 existed. Hence, PM was oxidized via at least two routes, one is the NO_2 route and another is non-NO_2 route, as shown below (Eq. 12). Similarly, NO was removed via reduction to N_2 and oxidation to NO_2, which is further reduced by PM or used to produce HNO_2 and HNO_3 (Eq. 13)

$$C_xH_y \rightarrow \left[\begin{array}{l} \xrightarrow{NO_2} C_{x-1}H_y - C(NO_2) \rightarrow C_{x-1}H_y + CO + NO \\ \\ \xrightarrow{O^*} C_{x-1}H_y + CO + CO_2 \end{array} \right. \tag{12}$$

$$NO \rightarrow \left[\begin{array}{l} \xrightarrow{\text{Plasma reduction}} N_2 \\ \\ \xrightarrow{\text{Plasma oxidation}} NO_2 \rightarrow \left[\begin{array}{l} \xrightarrow{C_xH_y} C_{x-1}H_y - C(NO_2) \rightarrow C_{x-1}H_y + CO + NO \\ \\ \xrightarrow{H_2O,OH} HNO_2, HNO_3 \end{array} \right. \end{array} \right. \tag{13}$$

Kinetics of PM removal

In a space between the Al wire (coil on the Al_2O_3 tube) and Al_2O_3 surface nearby, the Al_2O_3 wire yielded electric fields when pulse voltage was applied. The PCSD occurred in such a space when a large enough pulse voltage was applied. This space was defined as a PCDS zone. In the PCDS zone, nitrogen and oxygen in the exhaust gases were activated to reactive radicals and species such as N, O, and ozone O_3 that contribute to PM removal by oxidation of hydrocarbons and NO_x reduction, as discussed earlier. Because the PCSD occurred over the Al_2O_3 surface, plus the fact that particulates could be adsorbed on the surface of the Al_2O_3 tube, the mechanism of PM removal includes at most possibly three main steps: (1) adsorption/desorption of PM on to the surface of the Al_2O_3 tube, (2) reactive species production by the PCSD, and (3) PM oxidation and NO_x reduction in or over the PCSD zone. The kinetic model of PM removal is then written as follows.

Step 1. Adsorption/desorption of PM on Al_2O_3 surface

$$PM + s \xrightarrow{k_1} PM_s \tag{14}$$

$$r_1 = k_1([PM] - \lambda[PM_s]) \tag{15}$$

$$PM_s \xrightarrow{k_2} PM + s \tag{16}$$

$$r_2 = k_2([PM] - \lambda[PM_s]). \tag{17}$$

Here, s in m^2 denotes the active surface area of the Al_2O_3 tube over the PCSD zone; s might be a function of P and F; for simplicity, s denotes a constant in this study; PM_s is the surface

PM on/over the PCSD zone; λ in 1/m is a constant of PM adsorption/desorption, $\lambda = [PM]^*/[PM_s]$, $[PM]^*$ is the equilibrium PM concentration in the gas at $[PM_s]$; [ ] indicates the time-averaged concentration in g/m^2 for surface concentration of PM_s or in g/m^3 for PM concentration in the diluted exhaust gases; and k_1 and k_2 in m/s are adsorption and desorption constants of PM on the PCSD zone of the Al_2O_3 surface, respectively.

Steps 2 and 3. Production of active oxygen species and oxidation of PM; PM adsorbed on the surface of Al_2O_3 is then oxidized to CO and CO_2 in and/or over the PCSD zone by active oxygen species O* such as O, O_3, and NO_2. The rate of PM_s oxidation is defined as a pseudo first order of PM_s concentration and α orders of energy injection rate (PF) for O* species production

$$\text{PMs} + \text{O*} \xrightarrow{k_3} \text{CO} + \text{CO}_2 \tag{18}$$

$$r_3 = k_3[PM_s](PF)^\alpha \tag{19}$$

Here, k_3 is a reaction constant in m/J, and α is equal to 1, as calculated later.

At a steady state, the rate of PM concentration change could be considered negligible

$$\frac{d[PM]}{dt} = 0 \tag{20}$$

Since $d[PM]/dt = r_1 - r_2 - r_3$, the concentration of PM_s is then obtained by solving Eqs. 15, 17, 19, and 20:

$$[PM_s] = \frac{(k_1 - k_2)[PM]}{(k_1 - k_2)\lambda + k_3(PF)^\alpha}. \tag{21}$$

The PM reaction rate is then written by

$$r_3 = \frac{(k_1 - k_2)k_3(PF)^\alpha[PM]}{(k_1 - k_2)\lambda + k_3(PF)^\alpha}. \tag{22}$$

The PM reaction rate could be generally defined as Eq. 23, where V in m^3/s is the flow rate of the reaction gases. From the integration of Eqs. 22 and 23, the PM concentration at the outlet of the DBD reactor is given by Eq. 24, where $[PM]_0$ is the PM concentration at the inlet of the DBD reactor, and τ is the resistance time of the reaction gases passing through the vacant space over the plasma discharge zone, about 0.26 s in this study. Then, the PM removal X is given in Eq. 25

$$r_3 = -\frac{Vd[PM]}{sdt} \tag{23}$$

$$[PM] = [PM]_0 \exp^{-(k_1-k_2)k_3(PF)^\alpha s\tau/V/((k_1-k_2)\lambda+k_3(PF)^\alpha)} \tag{24}$$

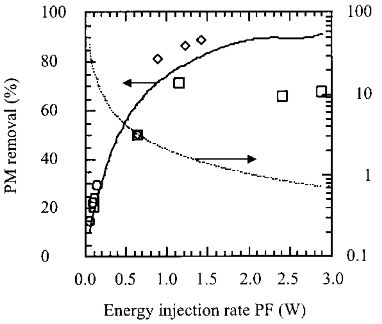

Figure 7. Comparison of simulation results and experimental results as a function of energy injection rate (PF) and γ values.

Symbols: ○: F fixed at 200 Hz; ◇: F fixed at 1 kHz; □: P fixed in a range of 6.6×10^{-4} to 8.1×10^{-4} J/pulse; ———: simulation results; · · · : γ values.

$$X = \frac{[PM]_0 - [PM]}{[PM]_0} = 1 - \exp^{-(k_1-k_2)k_3(PF)^\alpha s\tau/V/((k_1-k_2)\lambda+k_3(PF)^\alpha)}. \tag{25}$$

Since the PM removal rate X is proportional to the energy injection rate, PF, if $(k_1 - k_2)\lambda \gg k_3(PF)^\alpha$, Eq. 25 can be simplified as

$$X = \frac{[PM]_0 - [PM]}{[PM]_0} = 1 - \exp^{-k_3 s(PF)^a/(\lambda V)}. \tag{26}$$

Using the experimental results at 200 Hz and various energy injections, P, and least-square approximation, α was calculated to be 1.0. Equation 26 is then written as

$$X = 1 - \exp^{-m_1 \cdot m_2 PF/(m_1 + m_2 PF)}, \tag{27}$$

here

$$m_1 = \left((k_1 - k_2)\frac{s}{V}\tau\right), \qquad m_2 = \frac{k_3}{\lambda}\frac{s}{V}\tau.$$

Using the results shown in Figures 5 and 6 at pulse frequencies less than 3 kHz, simulation of PM removal was carried out as a function of the energy injection rate (PF) (Figure 7). Here m_1 and m_2 are 4.2 and 2.0, respectively. The simulation agreed with the experimental results at (PF) < 0.2 W, but with about 10% error at energy injection rates from 0.5 W to 1.5 W. Larger errors were found at energy injection rates higher than 1.5 W. Those errors are due to such factors as (1) the increase in surface temperature of the Al_2O_3 tube, which influences the λ value, and (2) the increase in the s value at a high energy injection rate.

From Eq. 27, the values of $\gamma = m_1/(m_2 PF)$ in [J m/s^3] correspond to the ratio of the net PM deposition ability to the PM removal ability. These γ values are also illustrated in Figure 7. At energy injection rates of less than 0.2 W, the γ value was higher than 10, which implied that under this condition, PM removal was mainly due to the energy injection rate. Conversely, at energy injection rates higher than 2 W, the γ

value was between 0.7 and 1, indicating that both PM adsorption and PCSD contribute to PM removal.

Conclusions

Removal of diesel PM and NO_x using PCSD and the DBD reactor were investigated at atmospheric pressure and with no external heating except plasma heating. NO_2 and active oxygen species were produced by PCSD. PM was oxidized to CO and CO_2 via the NO_2 route and the non-NO_2 route. NO was removed, possibly by reduction to N_2 and by oxidation to NO_2, with further reductions to HNO_2 and HNO_3. The mechanism of NO_x reduction will be clarified in detail in a future study.

PM removal was a function of PM adsorption and the energy injection rate. At a low energy injection rate of less than 0.2 W, PM removal was mainly proportional to the energy injection rate. At a high energy injection rate higher than 2 W, PM removal depended on both the adsorption rate and the energy injection rate.

The maximum PM removal was 89% at 1.42 W (Figure 7), with 40% NO_x removal. The PM removal ability under this condition was 9.0×10^{-8} g/J ($=(1.44 \times 10^{-7} \times 89\%)/1.42$). This suggested that a pulse power supply of 2.75 kW output power (about 5.1% of 54 kW (maximum output) of the diesel engine) is required for the removal of 89% PM emitted at a rate of 2.78×10^{-4} g/s (1 g/h). In this study, only the outside A1 coil electrode of the DBD reactor was used for PM removal. If two sides of electrodes could be used, the energy requirement could be improved down to about 1.4 kW. Further modifications of reactor structure and discharge condition are desirable for reducing the energy requirement.

Acknowledgment

The Ministry of Education, Culture, Sports, Science and Technology supported this study. One of the authors (S. Yao) is grateful to the New Energy and Industrial Technology Development Organization for a fellowship.

Literature Cited

Aoyagi, Y., "Present and Future Technologies for Reducing Exhaust Emissions in Diesel Engines," *Jidousya Gijyutsu,* **55**(9), 10 (2001).

Balmer, M. L., R. Tonkyn, S. Yoon, A. Kolwaite, S. Barlow, G. Maupin, and J. Hoard, "NOx Destruction Behavior of Select Materials When Combined with a Non-Thermal Plasma," Society of Automotive Engineers, Warrendale, PA (1999).

Chang, J. S., "Energetic Electron Induced Plasma Processes for Reduction of Acid and Greenhouse Gases in Combustion Flue Gas," *NATO ASI Ser.,* **34**(A), 1 (1993).

Chang, J. S., P. A. Lawless, and T. Yamamoto, "Corona Discharge Processes," *IEEE Trans. Plasma Sci.,* **19**(6), 1152 (1991).

Diesel Emission Control-Sulfur Effects (DECSE) Program, Phase I Interim Data, Report No. 1, Office of Transportation Technologies, http://www.ott.doe.gov/deces/pdfs/interim.pdf. (1999).

Diesel Emission Control-Sulfur Effects (DECSE) Program, Phase II Summary Report: NOx Adsorber Catalysts, Office of Transportation Technologies, http://www.ott.doe.gov/deces/pdfs/decse2final.pdf. (2000).

Diesel Emission Control-Sulfur Effects (DECSE) Program, Final Report: Diesel Oxidation Catalysts and Lean-NOx Catalysts, Office of Transportation Technologies, http://www.ott.doe.gov/deces/pdfs/decserpt.pdf. (2001).

Dorai, R., K. Hassouni, and M. J. Kushner, "Interaction Between Soot Particles and NOx During Dielectric Barrier Discharge Plasma Remediation of Simulated Diesel Exhaust," *J. Appl. Phys.,* **88**(10), 6060 (2000).

Dorai, R., and M. J. Kushner, "Consequences of Propene and Propane on Plasma Remediation of NOx," *J. Appl. Phys.,* **88**(6), 3739 (2000).

Dorai, R., and M. J. Kushner, "Effect of Propene on the Remediation of NOx from Engine Exhausts," Society of Automotive Engineers, Warrendale, PA (1999).

Dorai, R., and M. J. Kushner, "Repetitively Pulsed Plasma Remediation of NOx in Soot Laden Exhaust Using Dielectric Barrier Discharges," *J. Phys. D: Appl. Phys.,* **35,** 2954 (2002).

Eliasson, B., "Nonequilibrium Volume Plasma Chemical Processing," *IEEE Trans. Plasma Sci.,* **19**(6), 1063 (1991).

Hemmingway, M. D., D. Goulette, G. Ripley, T. Thoreson, J. Kupe, D. Herling, S. Basharan, M. Smity, D. Lessro, and J. Virden, "Evolution of a Non-Thermal Plasma System for Remediation of NOx in Diesel Exhaust," Society of Automotive Engineers, Warrendale, PA (1999).

Inomato, M., "Catalysts for Diesel Exhaust Treatment," *Eco-Industry,* **6**(2), 27 (2001).

Koltsakis, G. C., and A. M. Stamatelos, "Catalytic Automotive Exhaust Aftertreatment," *Prog. Energy Combust. Sci.,* **23,** 1 (1997).

Larkin, D. W., T. A. Caldwell, L. L. Lobban, and R. G. Mallinson, "Oxygen Pathways and Carbon Dioxide Utilization in Methane Partial Oxidation in Ambient Temperature Electric Discharges," *Energy Fuels,* **12**(4), 740 (1998).

Lepperhoff, G., D. Scharr, S. Pischinger, W. Neff, F. J. Trompeter, and K. Pochner, "Exhaust Emission Reduction of Combustion Engines by Barrier Discharge—A New Reactor/Generator System," Society of Automotive Engineers, Warrendale, PA (1999).

Liu, C. G., A. Marafee, B. J. Hill, G. H. Xu, R. Mallinson, and L. Lobban, "Oxidative Coupling of Methane with AC and DC Corona Discharges," *Ind. Eng. Chem. Res.,* **35**(10), 3295 (1996).

Lloyd, A., and T. Cackette, "Diesel Engines: Environmental Impact and Control," *J. Air Water Manage. Assoc.,* **51,** 809 (2001).

Matsui, Y., M. Hashimoto, A. Sakaguchi, K. Takashima, and A. Mizuno, "Oxidation of Carbon Soot Layer Using Pulsed Discharge Plasma," Society of Automotive Engineers, Warrendale, PA (2001).

Matsuura, T., "DPF as Diesel Particulate Removal Filter," *Nikkei Ecol.,* **6,** 39 (2000).

Neeft, J. P. A., M. Makkee, and J. A. Moulijn, "Diesel Particulate Emission Control," *Fuel Process. Technol.,* **47,** 1 (1996).

Penetrante, B. M., "Plasma Chemistry and Power Consumption in Non-Thermal deNOx," *NATO ASI Ser.,* **34**(A), 65 (1993).

Penetrante, B. M., R. M. Brusasco, B. T. Merritt, W. J. Pitz, G. E. Vogtlin, M. C. Kung, H. H. Kung, C. Z. Wan, and K. E. Voss, "Plasma-Assisted Catalytic Reduction of NOx," Society of Automotive Engineers, Warrendale, PA (1998).

Rappé, K. G., C. L. Aardahl, C. F. Habeger, D. N. Tran, M. A. Delgado, L.-Q. Wang, P. W. Park, and M. L. Balmer, "Plasma-Facilitated SCR of NOx in Heavy-Duty Diesel Exhaust," Society of Automotive Engineers, Warrendale, PA (2001).

Sano, N., H. Tamon, and M. Okazaki, "Removal of the Chlorofluorcabon 1,1,2-Tricholo-1,2,2-Trifluoroethane in Gas by a Corona-Discharge Reactor," *Ind. Eng. Chem. Res.,* **37**(4), 1428 (1998).

Tamon, H., H. Imanaka, N. Sano, and M. Okazaki, "Removal of Aromatic Compounds in Gas by Electron Attachment," *Ind. Eng. Chem. Res.,* **37**(7), 2770 (1998).

Tamon, H., H. Mizota, N. Sano, S. Schule, and M. Okazaki, "New Concept of Gas Purification by Electron Attachment," *AIChE J.,* **41**(7), 1701 (1995).

Tamon, H., N. Sano, and M. Okazaki, "Influence of Oxygen and Water Vapor on Removal of Sulfur Compounds by Electron Attachment," *AIChE J.,* **42**(5), 1481 (1996).

Thanyachotpaiboon, K., S. Chavadej, T. A. Caldwell, L. L. Lobban, and R. G. Mallinson, "Conversion of Methane to Higher Hydrocarbons in AC Nonequilibrium Plasmas," *AIChE J.,* **44**(10), 2252 (1998).

Thomas, S. E., A. R. Martin, D. Raybone, J. T. Shawcross, K. L. Ng, P. Beech, and J. C. Whitehead, "Non-Thermal Plasma Aftertreatment of Particulates, Theoretical Limits and Impact on Reactor Design," Society of Automotive Engineers, Warrendale, PA (2000).

Yao, S., E. Suzuki, and A. Nakayama, "Oxidation of Activated Carbon and Methane Using a High-Frequency Pulsed Plasma," *J. Hazard. Mater.,* **B83,** 237 (2001).

Zelenka, P., W. Cartellieri, and P. Herzog, "Worldwide Diesel Emission Standards, Current Experiences and Future Needs," *Appl. Catal. B: Environ.,* **10,** 3 (1996).

Manuscript received Mar. 14, 2003, and revision received June 26, 2003.